



## Carbon-Binder Optimization for Lithium-Ion Battery Extreme Fast Charge

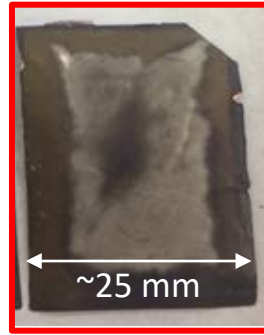
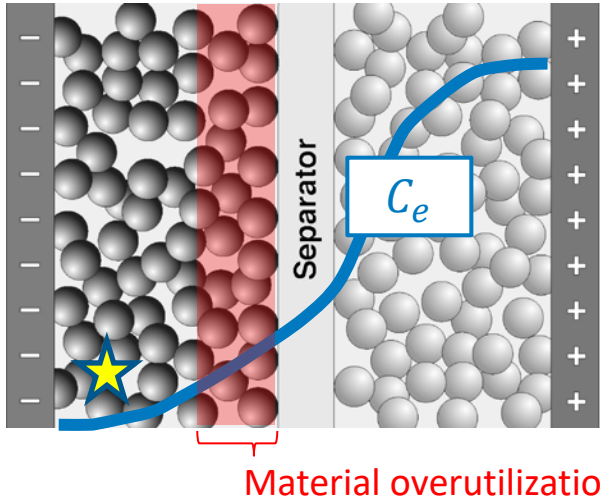
**Francois L. E. Usseglio-Viretta<sup>1</sup> Andrew M. Colclasure<sup>1</sup>, Alison R. Dunlop<sup>2</sup>, Stephen E. Trask<sup>2</sup>, Andrew N. Jansen<sup>2</sup>, Daniel P. Abraham<sup>2</sup>, Marco-Tulio F. Rodrigues<sup>2</sup>, Eric J. Dufek<sup>3</sup>, Tanvir R. Tanim<sup>3</sup>, Parameswara R. Chinnam<sup>3</sup>, Yeyoung Ha<sup>1</sup>, and Kandler Smith<sup>1</sup>**

<sup>1</sup> National Renewable Energy Laboratory, <sup>2</sup> Argonne National Laboratory, <sup>3</sup> Idaho National Laboratory

242<sup>nd</sup> ECS Meeting, Atlanta, 10 October 2022

- Background: achieving fast charging
- Impact of active material and carbon-black/binder domain (CBD) on tortuosity
- What is the optimal CBD loading ?
- Experimental and macroscale P2D modeling results on low and high CBD content cells

# Achieving fast charging

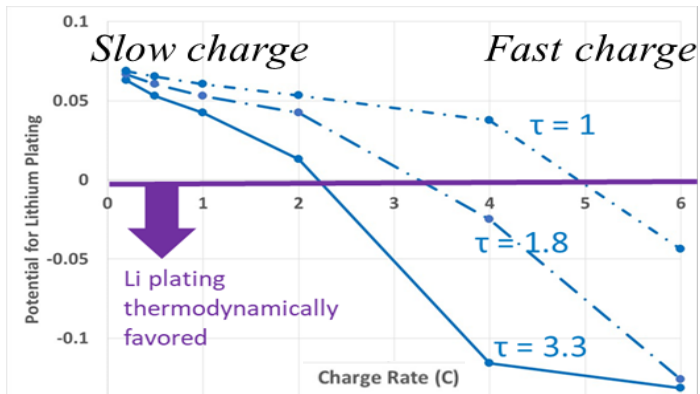


Post-mortem observation reveals material degradation due to over-utilization of the electrode at the electrode front

Photo: Eric Dufek and Tanvir Tanim, INL

**Deposition of lithium at the particle surface (Lithium plating) → capacity loss**

- Strong incentive to reduce tortuosity factor to enable fast charging without degradation.
- Although, it is one option among others.



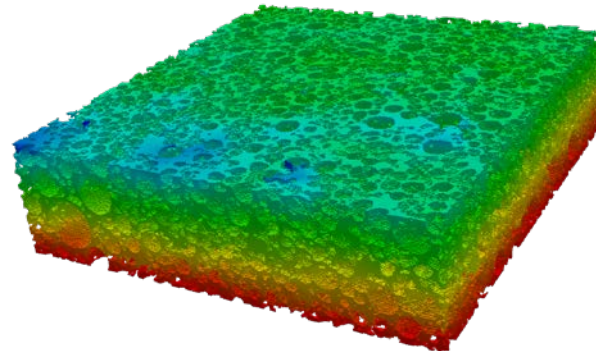
Electrolyte mass conservation

$$\frac{\partial \epsilon_e C_e}{\partial t} = \frac{\partial}{\partial x} \left( D^{eff} \frac{\partial C_e}{\partial x} \right) + \frac{1 - t_+^0}{F} j_{Li}$$

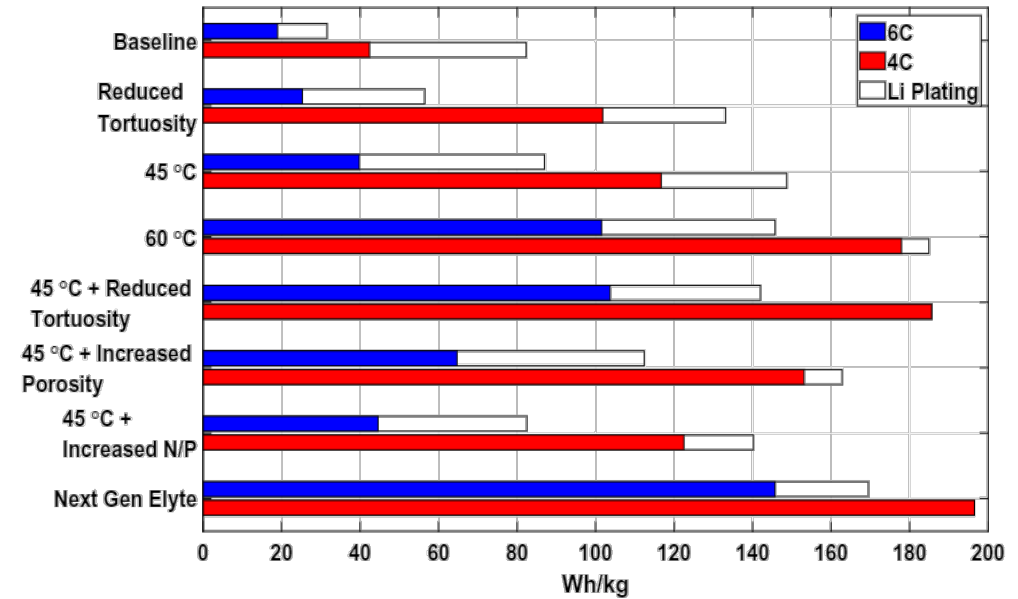
$$\frac{D^{eff}}{D^{bulk}} = \frac{\epsilon_e}{\tau}$$

A. M. Colclasure et al, JES, 166 8 A1412-A1424 (2019)

Predicted by macro-scale model, and linked to microstructure parameters



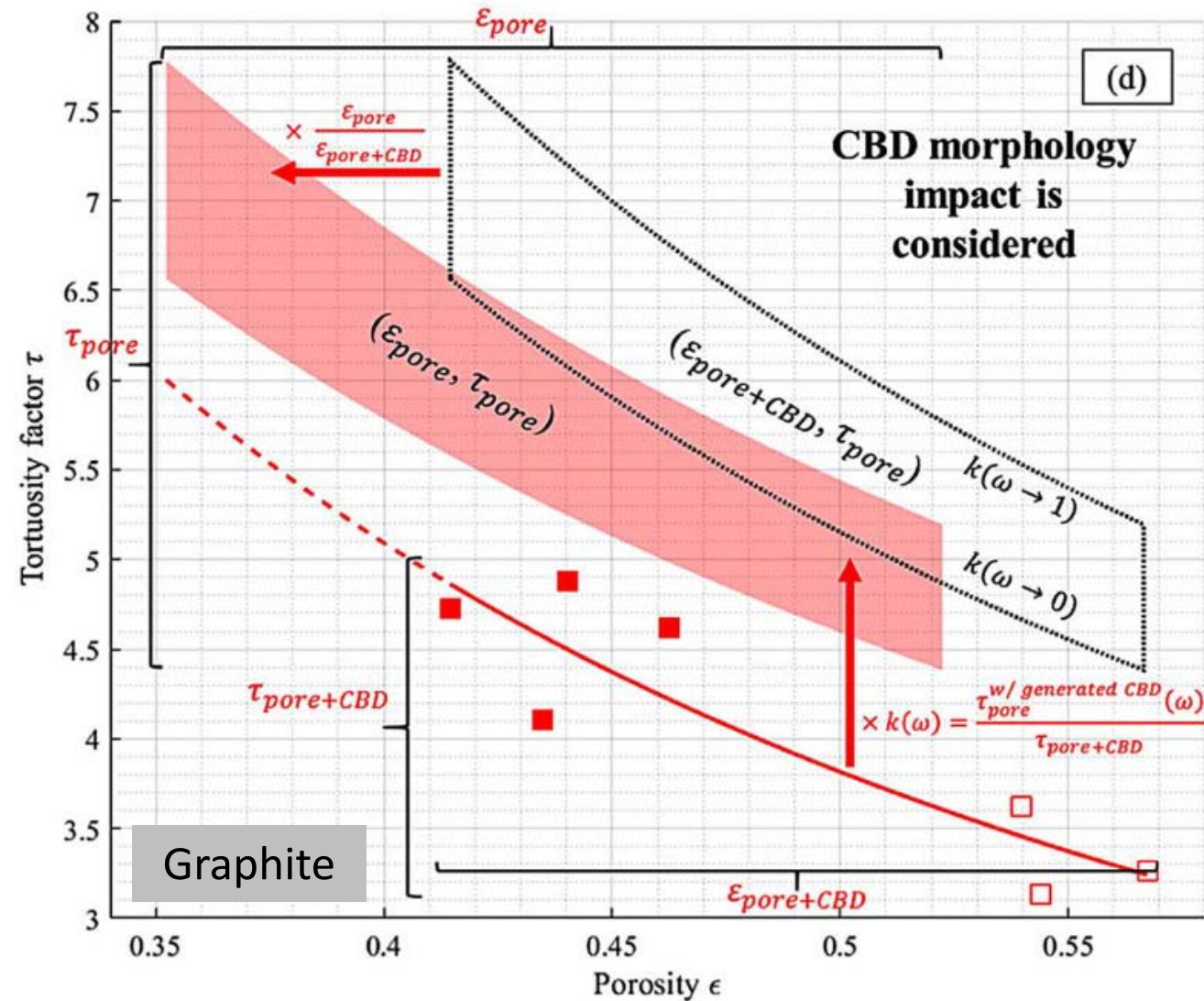
F. Usseglio-Viretta et al, ECS trans., 77 11 1095-1118 (2017)



A. M. Colclasure et al, Electrochimica Acta 337 (2020)



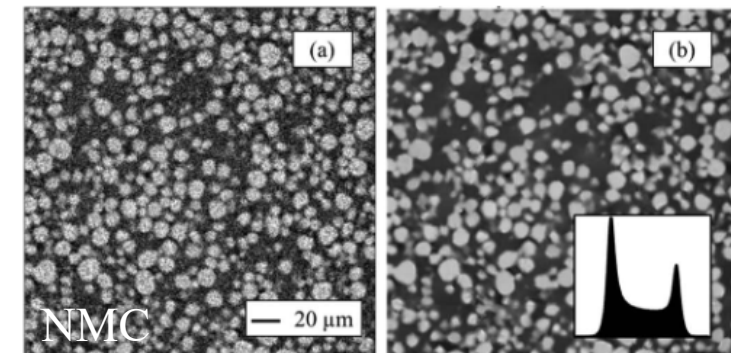
# Impact of active material and carbon-black binder (CBD) on tortuosity



Additives (carbon black, binder) induce a topology change resulting in an increment of the Bruggeman exponent.

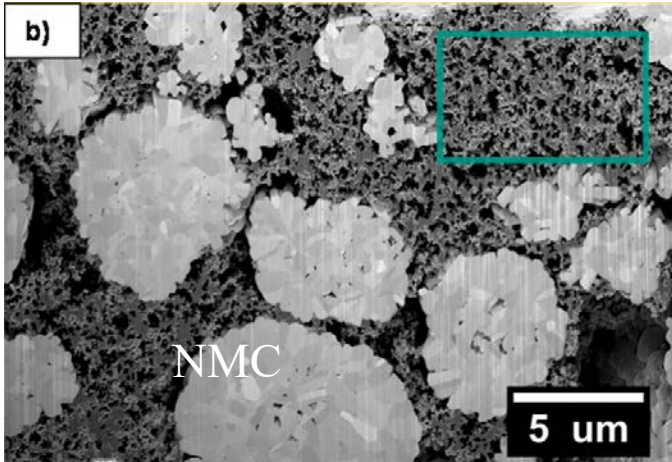
Transport penalty for a loading increase is higher for CBD than for active material.

Cells from Cell Analysis, Modeling and Prototyping (CAMP) facility at Argonne National Laboratory  
 NMC532 (90/5/5)  
 Graphite (92/2/6)

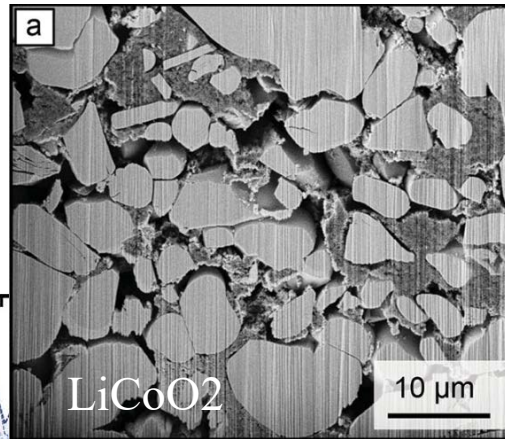


F. Usseglio-Viretta et al., Resolving the Discrepancy in Tortuosity Factor Estimation for Li-Ion Battery Electrodes through Micro-Macro Modeling and Experiment, J. Electrochem. Soc., 2018

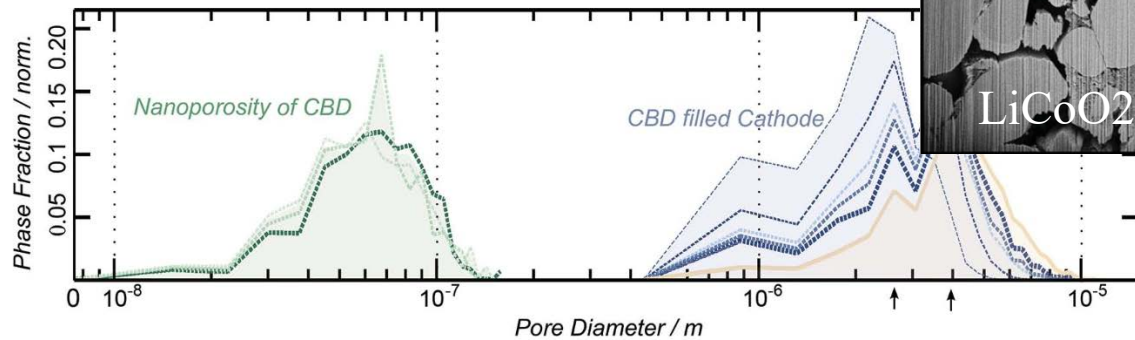
# CBD nanostructure and model representation



S. R. Daemi et al., ACS Appl. Energy Mater. 2018, 1, 8, 3702–3710

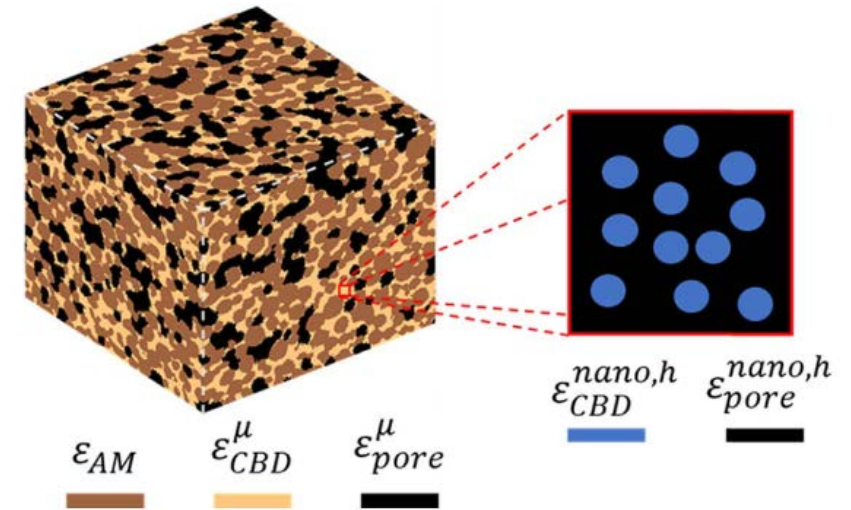


Zielke et al., Adv. Energy Mater. 2015, 5, 1401612



CBD nanopores range from 5 to 150 nm

**Our approach: X-ray CT large field of view with CBD numerically generated (heterogeneous distribution)**

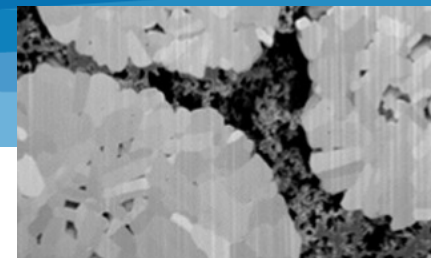


CBD voxel is homogenized (nanoporosity and effective electrolyte diffusivity) through reverse homogenization.  $p^{nano}$  is fitted until known macroscale electrolyte diffusivity is reached using microstructure

F. Usseglio-Viretta et al., Carbon-binder weight loading optimization for improved lithium-ion battery rate capability, J. Electrochem. Soc., 2022



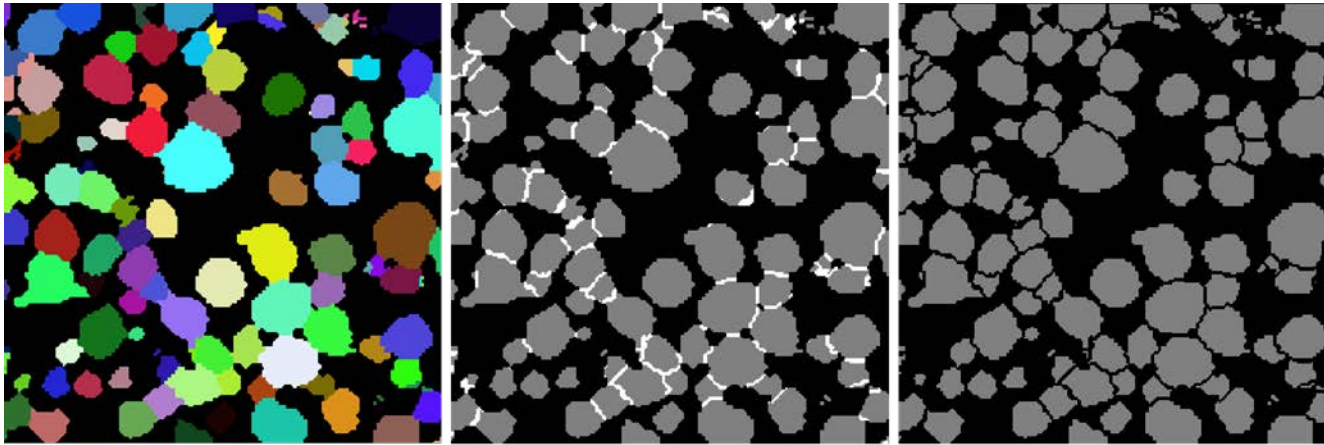
# Heterogeneous CBD distribution



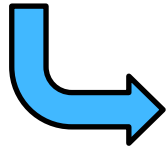
S. R. Daemi et al., ACS Appl. Energy Mater. 2018

Particles are connected through CBD in gaps between them

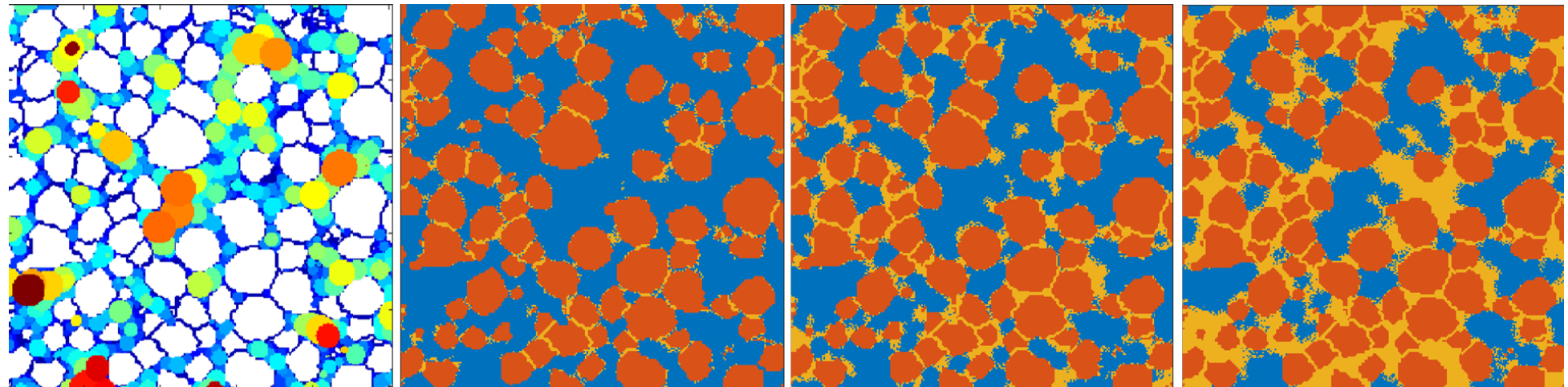
Cell manufacturing (ANL), X-ray CT imaging (UCL), then segmentation, particle identification, and separation (NREL)



10  $\mu$ m NMC



Open-source code with user-friendly GUI



c-PSD

$\epsilon_{CBD}^{\mu} = 0.05$

$\epsilon_{CBD}^{\mu} = 0.15$

$\epsilon_{CBD}^{\mu} = 0.25$

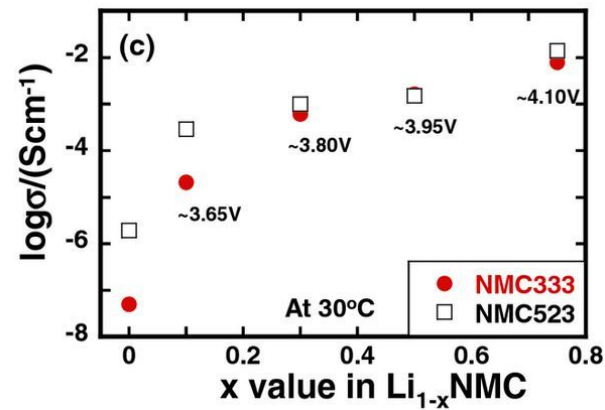
F. Usseglio-Viretta et al., Carbon-binder weight loading optimization for improved lithium-ion battery rate capability, J. Electrochem. Soc, 2022

F. Usseglio-Viretta et al., MATBOX: An Open-source Microstructure Analysis Toolbox for microstructure generation, segmentation, characterization, visualization, correlation, and meshing, SoftwareX, 2022

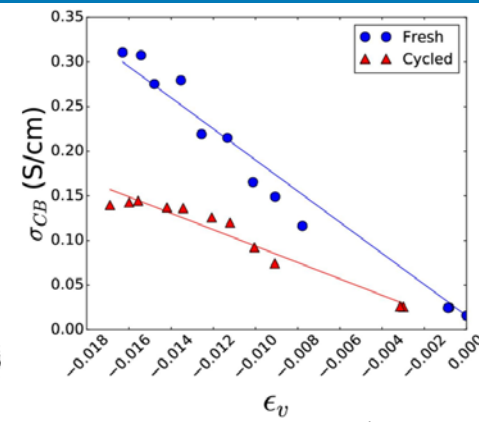
F. Usseglio-Viretta et al., Quantitative Relationships Between Pore Tortuosity, Pore Topology, and Solid Particle Morphology Using a Novel Discrete Particle Size Algorithm, J. Electrochem. Soc, 2020

# Different connectivities

- We know now how to represent/generate CBD.
- How to quantify it?



NMC523 at 30°C:  $\sim 1\text{e}^{-2}$  to  $1\text{e}^{-6}$   $\text{S cm}^{-1}$  for  $x=0.75$  and  $0.0$

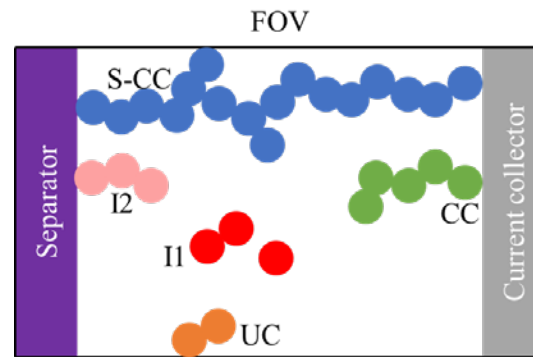


CBD: 0.02 to 0.3  $\text{S cm}^{-1}$  (**0.15  $\text{S cm}^{-1}$**  used in this work)

Electronic conductivity of (Left) NMC at different lithiation state, Amin et al., JES 2016 and (right) CBD for different volume strain, Trembacki et al., JES, 2017

Early classification of connectivity provided by Joos et al., JPS, 246 (2014): **connected**, **unknown** and **isolated** clusters

Proposed subclassification (I-IV) for the connected clusters to discriminate between different effective conductivities



### Connected clusters

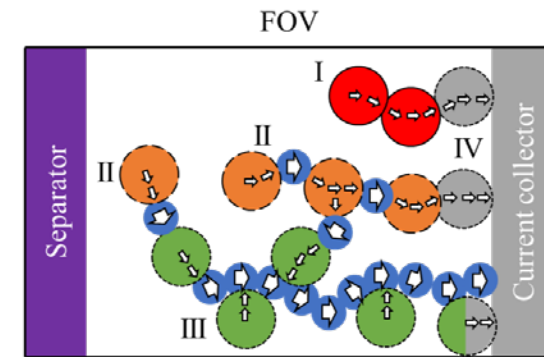
- Connected from separator to current collector (S-CC)
- Connected to current collector (CC)

### Unknown clusters

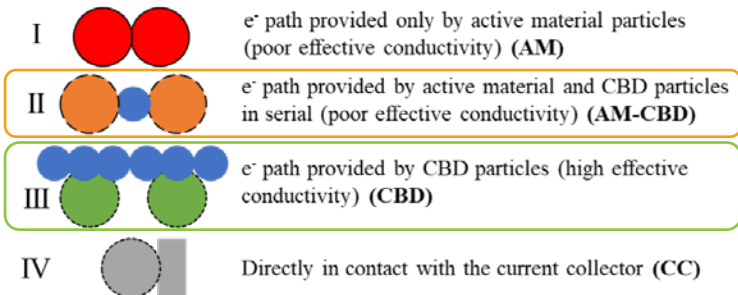
- Not connected, but located at the FOV's edges (UC)

### Isolated clusters

- Not connected to both separator and current collector (I1)
- Connected to separator, but not to current collector (I2)



- Active material particles (poor conductivity)
- CBD particles (high conductivity)



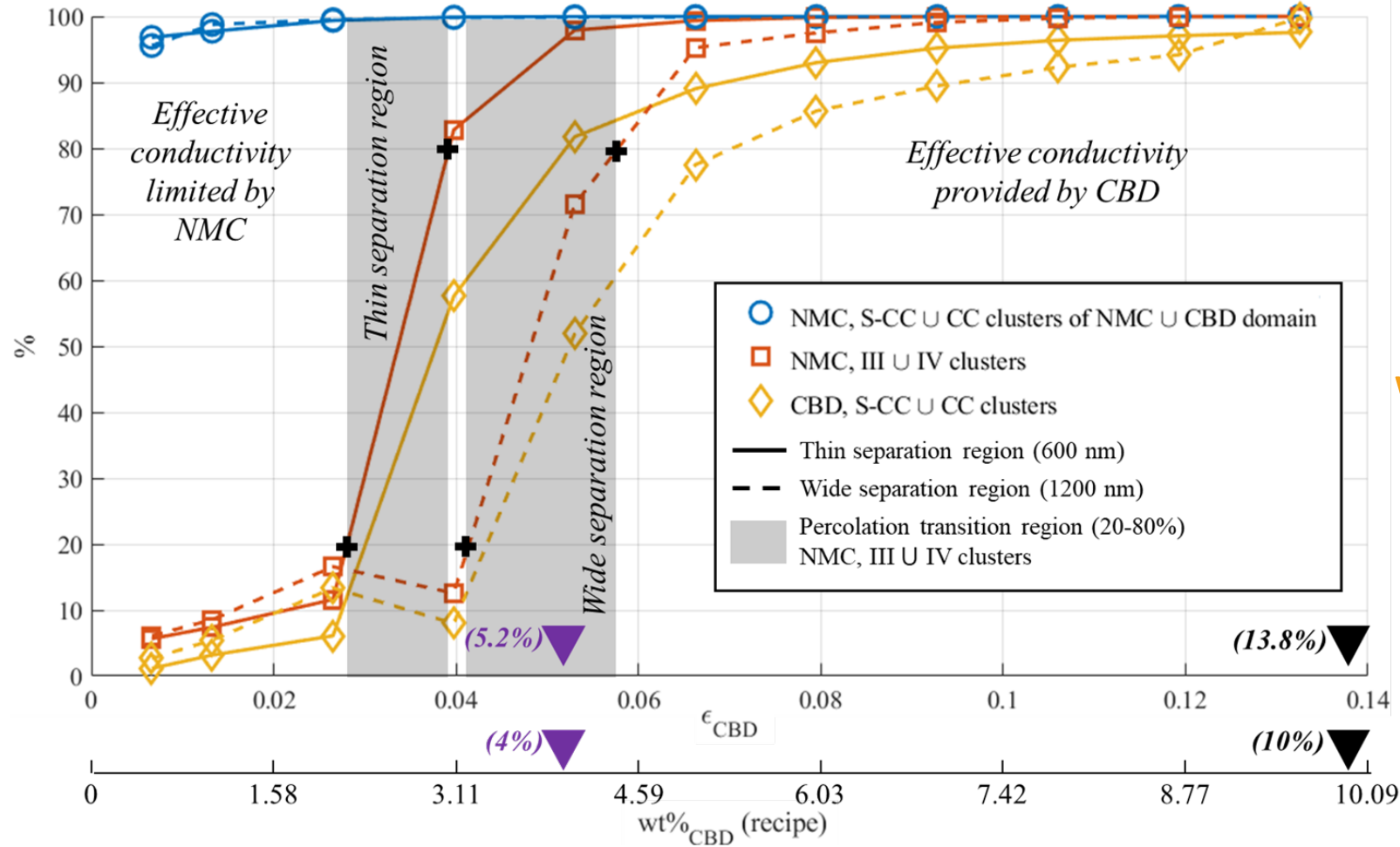
$$K_{eff}^{series} = \frac{\sum w_i}{\sum \frac{w_i}{K_i}}$$

To avoid

Desired connectivity

F. Usseglio-Viretta et al., Carbon-binder weight loading optimization for improved lithium-ion battery rate capability, J. Electrochem. Soc, 2022

# Percolation threshold... (NMC)

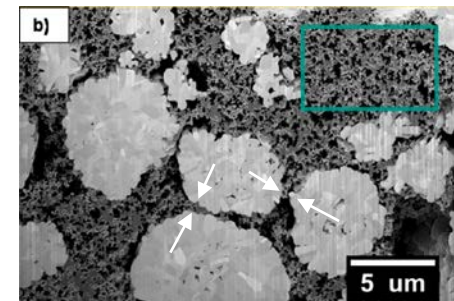
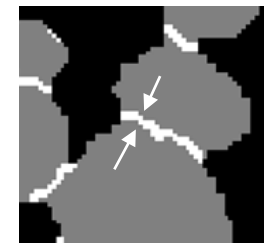


Percolation w/o constraint is achieved even with very little CBD

Desired connectivity requires ~3.9-5.8vol% (~2.9-4.2wt%) CBD

Which roughly corresponds to CBD percolation if considered alone

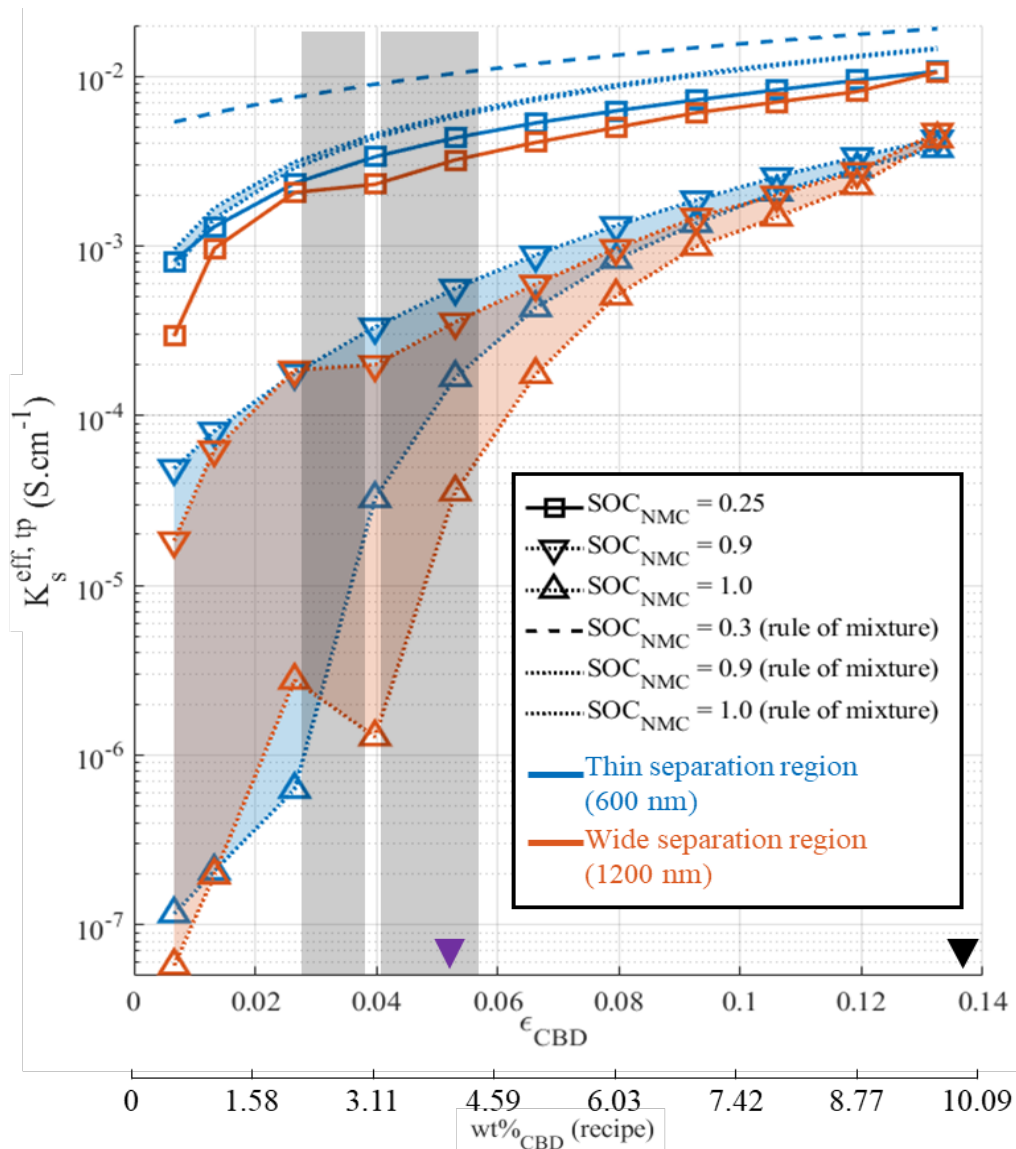
Percolation threshold calculated for a 'thin' (600 nm) and a 'wide' (1200 nm) separation region.



< 1  $\mu$ m



# ... and its impact on effective solid conductivity (NMC)



## High NMC conductivity (Li<sub>1-x</sub> NMC, x=0.75)

Incremental improvement, uncorrelated with percolation threshold, same trend as a rule of mixture

- For active material with high bulk conductivity (NMC at low lithiation, graphite), CBD only need to connect all particles together, no matter how



## Low NMC conductivity (Li<sub>1-x</sub> NMC, x=0.0, 0.1):



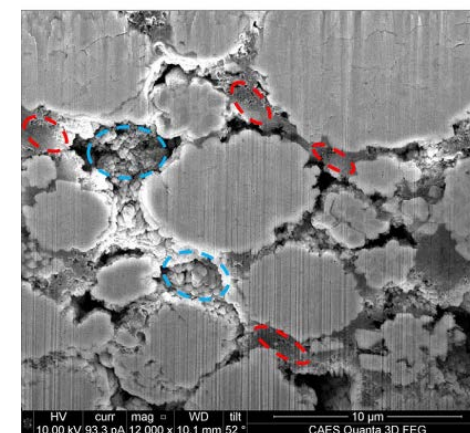
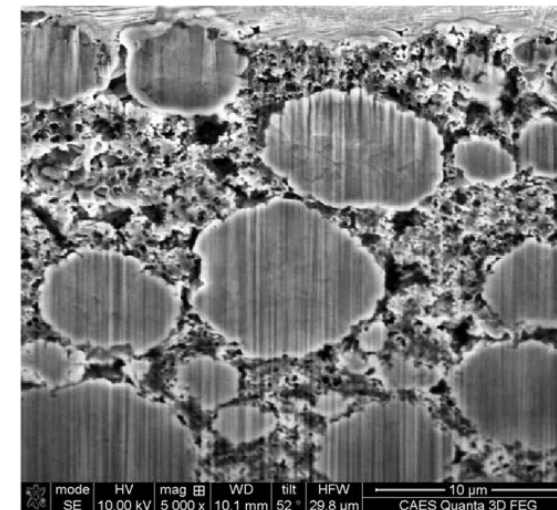
Sharp increase within percolation transition region, then more incremental (without a percolating CBD network, the effective conductivity is drastically limited by the poor NMC bulk conductivity).

Significant change from NMC near-full lithiation  $\nabla$  to NMC full lithiation  $\triangle$ : for low CBD loading, cathode effective conductivity at the end of discharge is expected to increase during cycling (due to loss of lithium at the anode side, i.e., SEI growth, that will prevent full re-lithiation at the cathode side)

# Experimentally investigated cells

Table III. Electrodes experimentally investigated.

			High CBD <sup>57</sup>	Low CBD
Anode (graphite)	Components (wt%)	Superior Graphite SLC1506T	91.83	95.83
		Timcal C45 carbon	2	0.5
		Kurcha 9300 PVDF	6	3.5
		oxalic acid	0.17	0.17
		Porosity (%)	38.2	37.4
		Coating loading (mg cm <sup>-2</sup> )	9.38	9.57
		Coating density (g cm <sup>-3</sup> )	1.34	1.37
		Coating thickness (μm)	70	70
		Cu foil thickness (μm)	10	10
		Total electrode thickness (μm)	80	80
Cathode (NMC532)	Components (wt%)	Reversible C/10; 0.005 to 1.5 V vs Li/Li <sup>+</sup>	2.98	3.05
		Toda NMC532	90	96
		Timcal C45 carbon	5	2
		Solvay Solef 5130 PVDF	5	2
		Porosity (%)	35.6	34.9
		Coating loading (mg cm <sup>-2</sup> )	18.57	17.24
		Coating density (g cm <sup>-3</sup> )	2.62	2.87
		Coating thickness (μm)	71	60
		Al foil thickness (μm)	20	20
		Total electrode thickness (μm)	91	80
Cell	N/P range	Reversible C/10; 3 to 4.2 V vs Li/Li <sup>+</sup>	2.54	2.54
		3 to 4.1 V	1.04 to 1.17	1.10 to 1.20



NMC532

# Expected beneficial impact on tortuosity (graphite)

Table IV. Anode microstructure ionic transport coefficients, experimentally measured with EIS, fitted in a macroscale P2D model, and calculated from microstructure analysis.

	EIS		P2D fit		Microstructure analysis	
	High CBD	Low CBD	High CBD	Low CBD	High CBD	Low CBD
$\epsilon_{pore}$	0.382	0.374	0.33	0.374	0.345	0.375
$\tau_{pore}^{tp}$	4.10 – 4.12	2.98 – 3.10	4.23	2.674	4.42	2.932
$\rho_{pore}^{tp}$	2.466 – 2.471	2.108 – 2.150	2.3	2.0	2.39	2.097
$N_M$	10.73–10.79	7.97–8.29	12.81	7.150	12.81	7.82

Reduce CBD loading, increase active material volume

Reduce CBD loading, keep active material volume constant

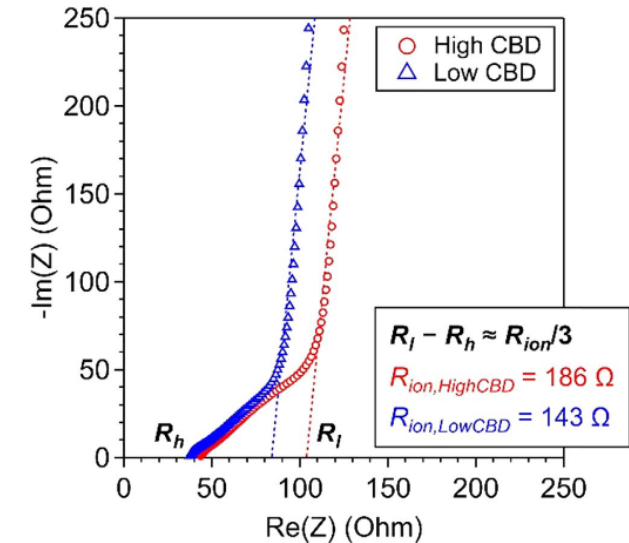


Figure 9. Nyquist plots of graphite/graphite symmetric coin cells containing 10 mM TBAClO<sub>4</sub> in EC/DMC (1:1, w/w) electrolyte. High and low CBD loading electrode results are shown with linear fits and calculated  $R_{ion}$  values.

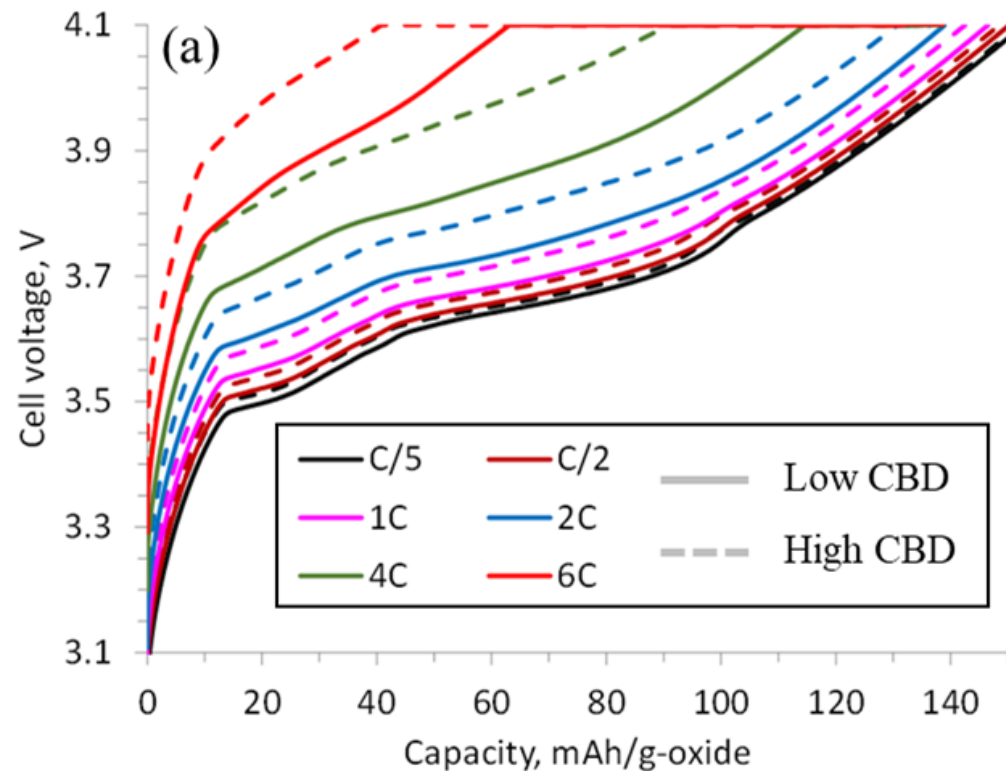
Bruggeman exponent is the most relevant metric for comparison as 3 cases does not have exactly the same porosity. All 3 cases agree on a -0.3 to -0.36 decrease.

- Experimental confirmation that a better electrolyte effective diffusion coefficient can be achieved by lowering the CBD loading, even though the porosity has been decreased
- Diffusion penalty of a CBD element of volume > diffusion penalty of an AM element of volume
  - **Volume fractions are all not the same**



# Rate capability at beginning of life

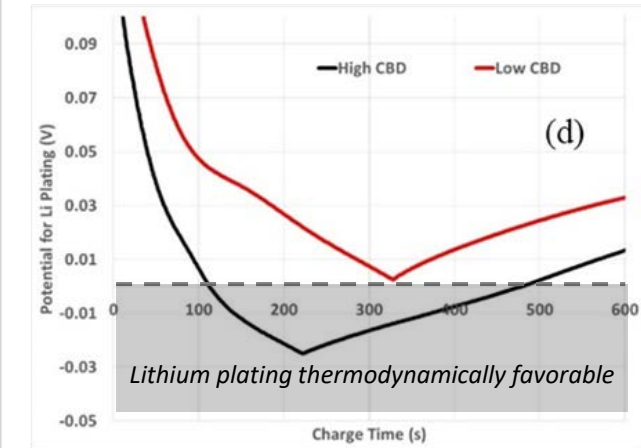
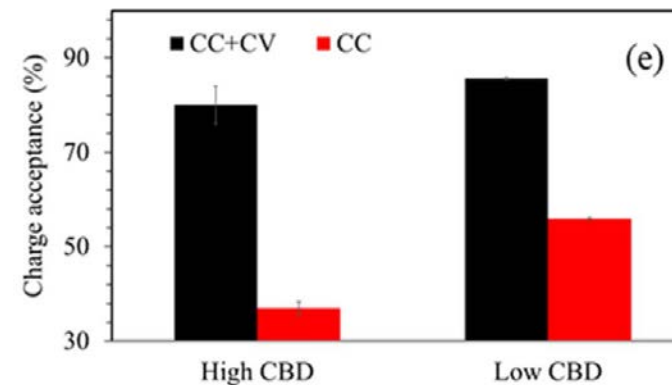
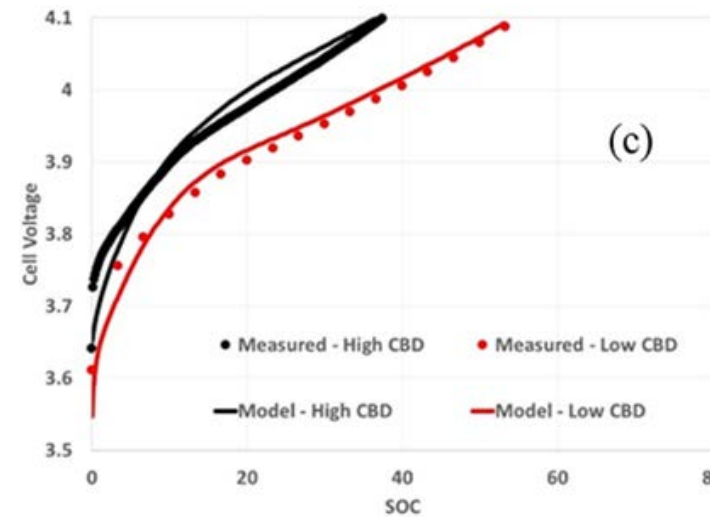
## Coin cells



Experimental voltage profiles for coin cells with the lower (solid lines) and higher (dashed lines) CBD contents, charged at various rates

- Higher capacity with larger gains measured for fast charging

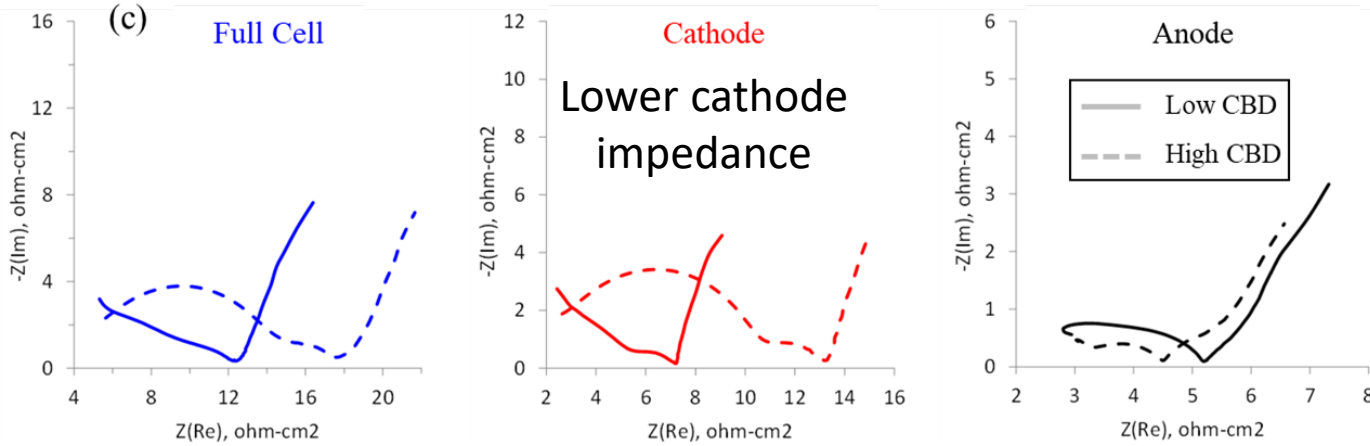
## Pouch cells



- Experiments and model are in good agreement.
- Model predicts no plating.
- 10 min 6C-CC-CV: SOC reached @4.1V cutoff was only 37% for cell with high CBD loading, and 55% with low loading

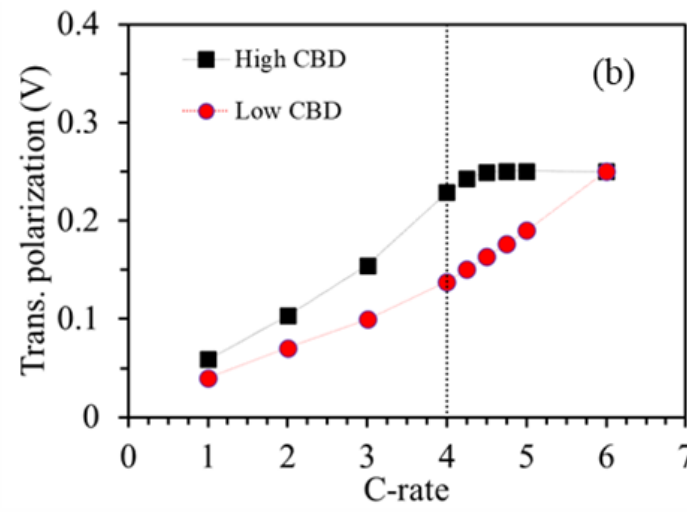
# Performance improvements due to

- Lower impedance (custom-3-electrode cells, EIS)

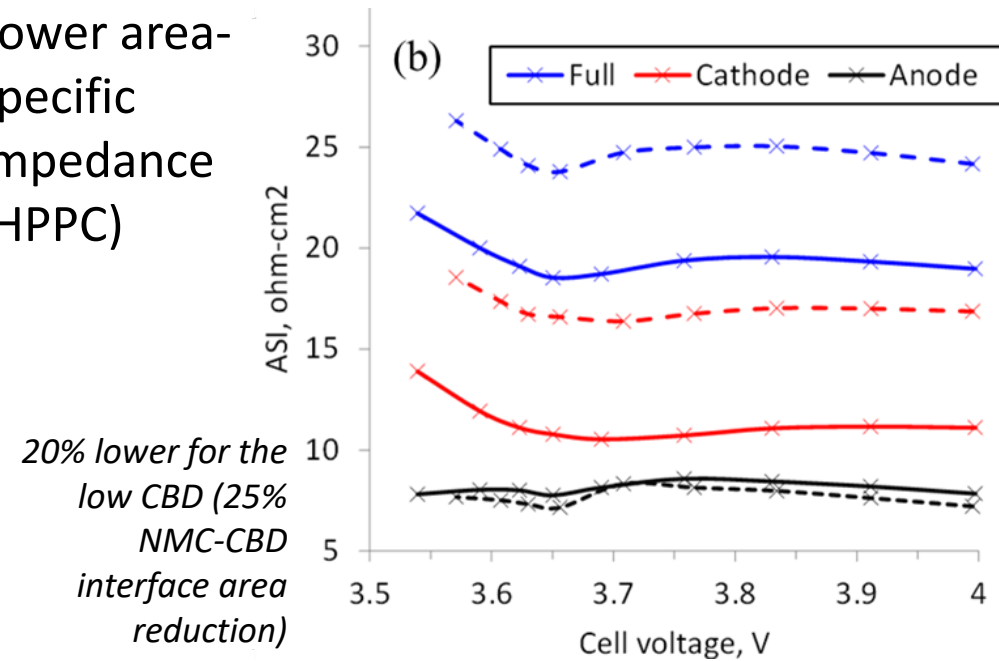


- Lower cell transport polarization (SLPC)

No more plateau  
(Li-plating marker)



- Lower area-specific impedance (HPPC)



Performance improvements are attributed to the reduced electrode tortuosity, cathode film resistance, and cathode thickness.

# Conclusions

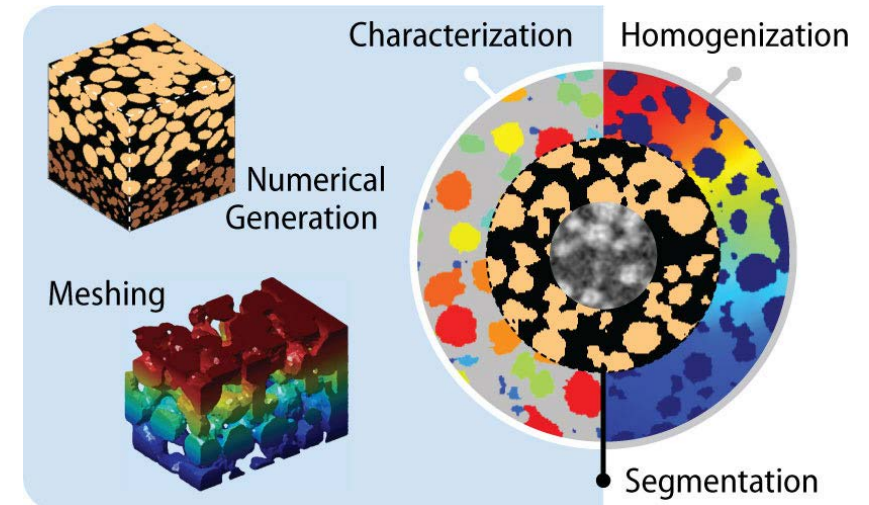
- **CBD impacts negatively effective diffusion, more than active material for the same volume**
  - Rebalancing loading between active material and CBD can improve effective diffusivity even with a lower porosity
  - **Anode: 8wt% - 4wt% CBD → Bruggeman exponent reduction ~2.5 to ~2.1**
  - **Cathode: 10wt% - 4wt% CBD → Bruggeman exponent reduction ~2.0 to ~1.8**
- High CBD loading are not required to achieve desired percolation (**cathode: ~3.9-5.8vol%, ~2.9-4.2wt% CBD loading**).
- Impact of CBD loading on solid conductivity:
  - **10wt% CBD:  $K_{eff}^{NMC}$  almost insensitive with NMC lithiation:  $0.5e^{-2}$  to  $1e^{-2}$  S.cm<sup>-1</sup>**
  - **4wt% CBD:  $K_{eff}^{NMC}$  dependent with NMC lithiation: low lithiation (0.25):  $3.5e^{-3}$  S.cm<sup>-1</sup>, near maximum lithiation (0.9):  $3.5e^{-4}$  -  $5.5e^{-4}$  S.cm<sup>-1</sup>, full lithiation (1.0):  $0.3e^{-4}$  –  $1.6e^{-4}$  S.cm<sup>-1</sup>**
- Higher polarization for high CBD content cells for charging rate >1C. **Single layer Pouch cell capacity improvement: from 37% (80%) to 55% (86%), respectively for high and low CBD cells at the cutoff voltage (and at the end of the 10 min 6C CC-CV). Model predicts no lithium plating.**
- **Area-specific impedance (electrochemical impedance spectroscopy) 20% lower for low CBD cell, mostly attributed to lower cathode impedance.** In agreement with hybrid pulse power characterization measurement, and coherent with the 25% NMC-CBD interface area reduction.
- Low loading increases **risk of delamination**, especially anode side. Recommendation based on cycling experiment: **keep 8wt% loading for graphite but reduce to 4wt% for cathode**



# References and acknowledgements

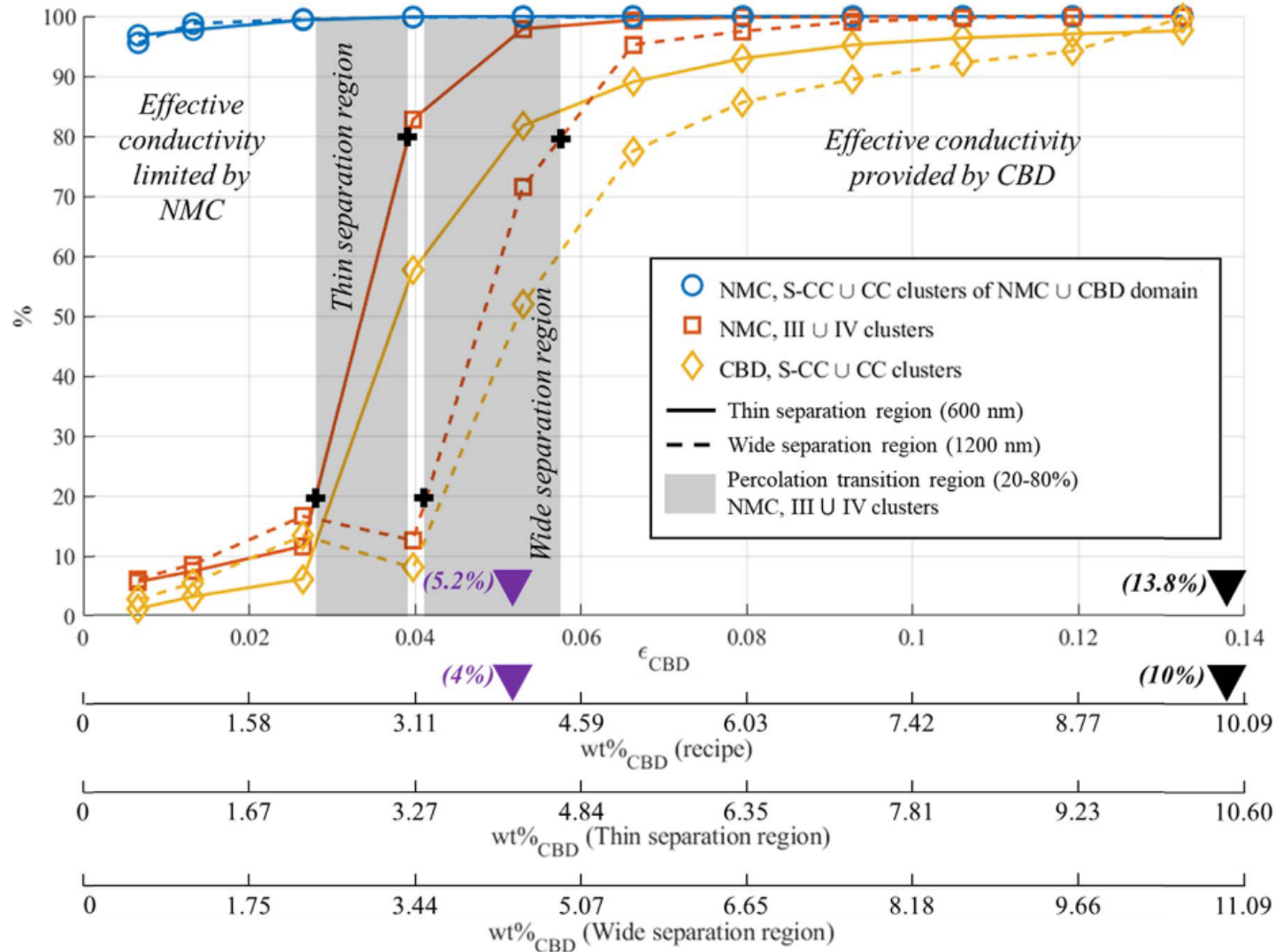
- **Impact of carbon-black binder loading and CBD numerical generation:**
  - Francois L. E. Usseglio-Viretta et al., *Carbon-Binder Weight Loading Optimization for Improved Lithium-Ion Battery Rate Capability*, Journal of The Electrochemical Society, 169 070519, **2022**, <https://doi.org/10.1149/1945-7111/ac7ef9>
- **Particle identification method:**
  - Francois L. E. Usseglio-Viretta et al., *Quantitative Relationships Between Pore Tortuosity, Pore Topology, and Solid Particle Morphology Using a Novel Discrete Particle Size Algorithm*, Journal of The Electrochemical Society, 167 100513, **2020**, <https://doi.org/10.1149/1945-7111/ab913b>
- **Carbon-black binder volume is more detrimental than active material (NMC, Graphite) for effective electrolyte diffusion:**
  - Francois L. E. Usseglio-Viretta et al., *Resolving the Discrepancy in Tortuosity Factor Estimation for Li-Ion Battery Electrodes through Micro-Macro Modeling and Experiment*, Journal of The Electrochemical Society, 165 (14) A3403-A3426, **2018**, <https://doi.org/10.1149/2.0731814jes>
- **Macroscale fast-charging modeling:**
  - Andrew M. Colclasure et al., *Electrode scale and electrolyte transport effects on extreme fast charging of lithium-ion cells*, Journal of The Electrochimica Acta, 337, **2020**, <https://doi.org/10.1016/j.electacta.2020.135854>
  - Andrew M. Colclasure et al., *Requirements for Enabling Extreme Fast Charging of High Energy Density Li-Ion Cells while Avoiding Lithium Plating*, Journal of The Electrochemical Society, 166 8, **2019**, <https://doi.org/10.1149/2.0451908jes>
- **Microstructure-related algorithms used in this work are open-source and available at:**
  - Francois L. E. Usseglio-Viretta et al., *MATBOX: An Open-source Microstructure Analysis Toolbox for microstructure generation, segmentation, characterization, visualization, correlation, and meshing*, SoftwareX 17 100915, **2022**, <https://doi.org/10.1016/j.softx.2021.100915>
  - NREL webpage: <https://www.nrel.gov/transportation/matbox.html>

- Support for this work from US Dept. of Energy, Office of Vehicle Technologies Energy Storage Program
- Extreme fast Charge and Cell Evaluation (XCEL) DOE Project
- Project Manager: Samuel Gillard



Additional slides

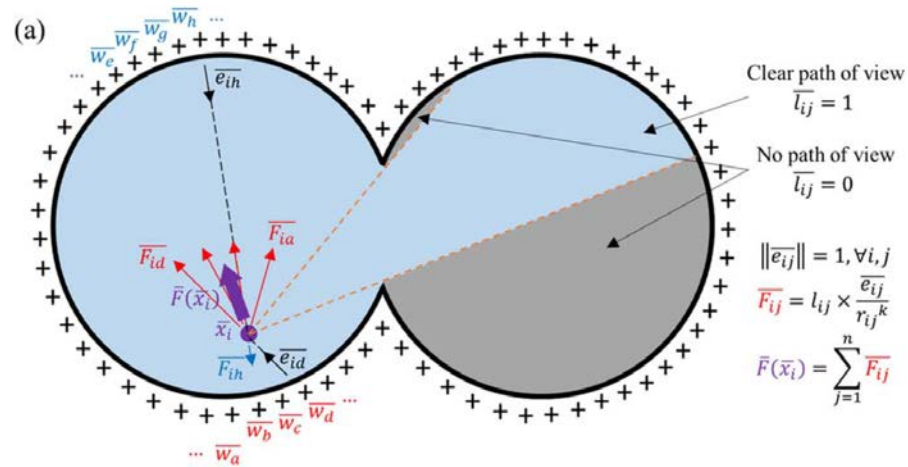
# Particle separation impact on volume fractions



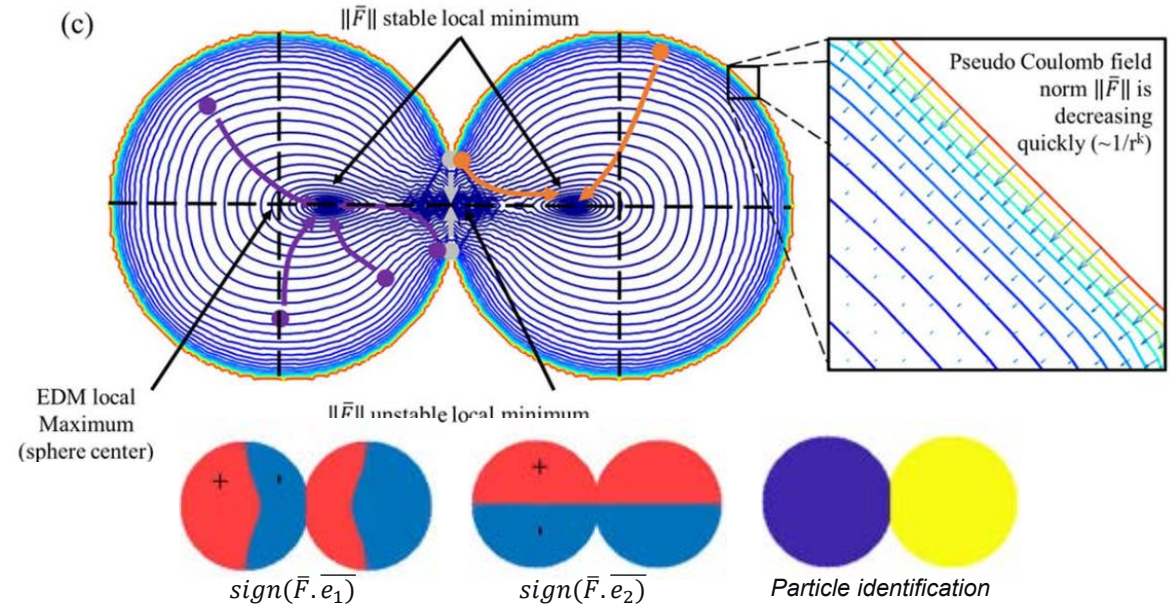
Slight shift in volume fractions/loading due to particle isolation



# Particle identification



**Pseudo-Coulomb repulsive field (PCRF) method**



F. Usseglio-Viretta et al., *MATBOX: An Open-source Microstructure Analysis Toolbox for microstructure generation, segmentation, characterization, visualization, correlation, and meshing*, SoftwareX, 2022

F. Usseglio-Viretta et al., *Quantitative Relationships Between Pore Tortuosity, Pore Topology, and Solid Particle Morphology Using a Novel Discrete Particle Size Algorithm*, J. Electrochem. Soc., 2020

**Almost zero-over-segmentation compared with baseline watershed method**

